

# Gameplay Filters: Safe Robot Walking through Adversarial Imagination

Duy P. Nguyen<sup>\*§</sup>, Kai-Chieh Hsu<sup>\*§</sup>, Wenhao Yu<sup>†</sup>, Jie Tan<sup>†</sup>, Jaime F. Fisac<sup>\*</sup>

<sup>\*</sup>Department of Electrical and Computer Engineering, Princeton University, United States

{duyn, kaichieh, jfisac}@princeton.edu

<sup>†</sup>Google Deepmind, United States

{magicmelon, jietan}@google.com

*Abstract*—Ensuring the safe operation of legged robots in uncertain, novel environments is crucial to their widespread adoption. Despite recent advances in safety filters that can keep arbitrary task-driven policies from incurring safety failures, existing solutions for legged robot locomotion still rely on simplified dynamics and may fail when the robot is perturbed away from predefined stable gaits. This paper presents a general approach that leverages offline game-theoretic reinforcement learning to synthesize a highly robust safety filter for high-order nonlinear dynamics. This *gameplay filter* then maintains runtime safety by continually simulating adversarial futures and precluding task-driven actions that would cause it to lose future games (and thereby violate safety). Validated on a 36-dimensional quadruped robot locomotion task, the gameplay safety filter exhibits inherent robustness to the sim-to-real gap without manual tuning or heuristic designs. Physical experiments demonstrate the effectiveness of the gameplay safety filter under perturbations, such as tugging and unmodeled irregular terrains, while simulation studies shed light on how to trade off computation and conservativeness without compromising safety.

## I. INTRODUCTION

Increasingly, autonomous robots are being deployed beyond controlled environments and required to operate reliably in uncertain, unforeseen conditions [1–5]. This has resulted in a growing need for robot safety frameworks that can scale with system complexity and generalize gracefully to novel environments.

Model-based approaches developed by the robotics and control communities offer a principled treatment of safe decision-making under uncertainty. Unfortunately, computing global safety fallback strategies for high-dimensional, nonlinear robot dynamics remains an open problem. State-of-the-art numerical safety methods only scale to 5–6 state variables [6, 7], woefully short of the 12 needed to accurately model the flight of a drone in free space, let alone the 30–50 required for most legged robots. Analytical approaches like Lyapunov controllers and CBFs rely on hand-design, structural assumptions, and reduced-order models [8, 9], restricting their use to a local operating envelope, such as a predefined stable walking gait. As a result, legged robots are notorious for falling easily, especially on irregular terrain or when externally perturbed (pushed, tugged, or tripped).

Data-driven approaches grounded in machine learning address the scalability challenge by automatically distilling

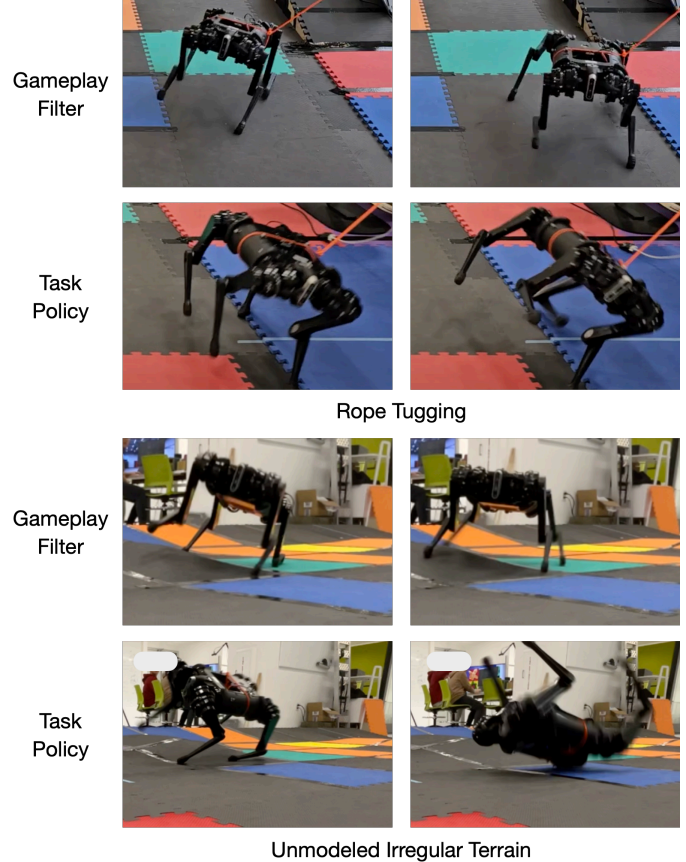


Fig. 1: We deploy our gameplay-based safety filter on a quadruped robot equipped with a safety-agnostic walking (task) policy, and evaluate its effectiveness under strong tugging forces and unmodeled irregular terrain. The *gameplay filter* continually monitors the robot’s safety by rapidly simulating adversarial futures, pitting its best-effort safety strategy against a learned virtual adversary that aims to exploit uncertainty and sim-to-real error to make it tip over. If hazardous conditions arise, the filter intervenes to preclude task-driven actions that would cause the robot to lose this imaginary safety game at a later time. Interventions result in highly robust, adaptive behaviors such as counterbalancing to fight persistent pulls and springing into a wide stance to break imminent falls.

<sup>§</sup>Denotes equal contribution.

efficient representations from the robot’s prior experience or, more recently, from web-scale data [10]. In practice, however, learned models for robot control, including deep reinforcement learning and imitation learning, are often trained in simulated environments due to hardware constraints and poor sample complexity (requiring millions of training episodes that can much more easily be procured by at-scale simulation). The discrepancy between training and deployment conditions, or *sim-to-real gap*, can result in deteriorated operational performance and, in extreme cases, catastrophic safety failures (e.g., damaging the robot or hurting nearby people) [3]. Additionally, end-to-end approaches often require re-training for different task specifications, which presents technical challenges in balancing safety objectives with task-specific goals, especially avoiding situations where a robot may unexpectedly prioritize task performance over safety.

A recent line of work breaks down the safety–performance trade-off through variations of a supervisory control mechanism known as a *safety filter*, which monitors the autonomous system’s safety at runtime and intervenes when necessary by adjusting the original performance-oriented control to avert catastrophic failures [11–16]. While some efforts have been made to synthesize safety filters for legged robot locomotion, these typically rely on simplified low-order dynamics to maintain tractability, and they lack a systematic treatment of uncertainty and reality gap [3, 17].

This paper introduces a novel type of safety filter that brings together the scalability of learning-based representations and the reliability of model-based safety analysis, enabling highly robust and minimally disruptive safety assurance for arbitrary robot task policies. Unlike most general safety filter techniques, the approach scales readily to robot dynamics with tens of state dimensions, which allows us to focus on its use in the dynamic legged locomotion domain. Further, our safety filter can monitor a closed-loop policy and address the associated computational latency, while existing safety filters only handle a single control input.

A preliminary offline stage leverages game-theoretic reinforcement learning to synthesize control and disturbance policies, which can be systematically used to construct safety filters for general nonlinear, high-dimensional dynamic systems at runtime. At every control cycle, the online gameplay safety filter assesses safety risks based on an imagined game between the control and adversarial disturbance policy trained in offline gameplay learning. This imagined gameplay aims to simulate the worst-case realization of the uncertainty in the system, either from a sim-to-real error or perturbations from the environment. If dangerous conditions emerge, the filter steps in to prevent task-driven actions that could lead the robot to lose in the subsequent safety-oriented gameplay.

The effectiveness of the proposed gameplay safety filter is validated in a legged robot locomotion task with a 36-dimensional state space and a 12-dimensional control

space.<sup>1</sup> Our results demonstrate that the gameplay safety filter is inherently robust to the sim-to-real gap, operating in a “zero-shot” manner without requiring manual design or hyperparameter tuning during deployment. Moreover, the gameplay safety filter achieves a high safety rate without being overly conservative, avoiding frequent interventions in the performance-oriented control policy. Importantly, the gameplay safety filter synthesis remains independent of the performance-oriented policy, making it modular and adaptable to any performance-oriented policy at runtime. Our evaluation includes real-world experiments on different terrains with perturbations (see Fig. 1) and a comprehensive simulation study on the relative importance of design choices.

## II. RELATED WORK

**Learning for Locomotion.** Conventionally, legged locomotion has been addressed through model-based techniques, including model-predictive control [18] and trajectory optimization [19]. However, recent advancements in deep learning offer the opportunity to learn directly from interactions with environments and feedback in the form of a reward signal, bypassing the need for intricate dynamics modeling and extensive domain knowledge. Kostrikov et al. [5] demonstrated the direct training of locomotion policies across various terrains in the real world through reinforcement learning by carefully formulating the problem with consideration for state space, action space, and reward function. Despite the success of reinforcement learning, it relies on trial and error during training. In safety-critical environments, learning from scratch can lead to catastrophic safety failures. An alternative approach involves initially training control policies in simulation and then bridging the simulation-to-real gap through methods such as domain randomization [20], task-driven adaptation [1, 21], and system identification [22].

**Safety Filters.** While learning-based policies discussed earlier exhibit practical utility, they primarily focus on task-oriented performance metrics. However, ensuring their safe operation in unforeseen, uncertain, and unforgiving environments is of paramount importance. A recent line of work aims at inducing safety awareness and even guarantees for learning-based policies through a *safety filter*. The runtime operation of every safety filter can be conceptualized as two interrelated functions: *monitoring* and *intervention* [11]. The safety filter continually monitors the robot’s planned actions to assess the level of safety risk. Subsequently, the filter may intervene by modulating or entirely overriding the robot’s intended control input to guarantee the preservation of safety. Many safety filters incorporate monitoring and intervention procedures guided by a safety-oriented control strategy, which the filter views as a viable *fallback*.

One important family of safety filters is built on Hamilton-Jacobi (HJ) reachability analysis, which computes a global safe value function through dynamic programming [23, 24]. The

<sup>1</sup>See <https://saferobotics.princeton.edu/research/gameplay-filter> for supplementary material.

resulting value function encodes the maximal safe set and optimal safety fallback, and thus, a *least-restrictive* safety filter can be synthesized by a *switch-type* intervention [12]. Although systematic and powerful, HJ methods have poor scalability and are limited to no more than 6 state dimensions [25].

On the other hand, control barrier functions (CBFs) [13, 26] no longer encode or approximate the maximal safe set. Instead, CBFs, if found, provide a sufficient condition to keep the system safe forever, akin to control Lyapunov functions [27]. Another critical feature of CBFs is their usage of *optimization-type* intervention, which finds minimal modulation to the task-oriented control that still keeps the system safe, and thus CBFs allow a smooth intervention mechanism. However, finding a CBF for general dynamics is usually not trivial, and CBF is only local and not robust to model mismatch.

For high-dimensional dynamics, computing global optimal value functions (HJ) is computationally prohibitive, and finding a valid CBF is often heuristic. Instead of relying on value functions, model predictive safety filters aim to certify the system safety in real time by forward simulating (“rolling out”) or trajectory optimization,<sup>2</sup> [14, 15, 29] which closely link to this work. Hsu et al. [29] consider the forward-reachable set (FRS) of the system trajectories. However, the use of FRS brings two challenges for general high-dimensional dynamics: 1) FRS needs to be tight to make safety filters not overly conservative, and 2) the computation of FRS needs to be quick to satisfy real-time constraints. Instead, Bastani and Li [15] assume disturbance distribution is known, by which a sufficient number of trajectories are sampled and a statistical guarantee is derived; nonetheless, disturbance distribution may be difficult to obtain in practice.

Safety filters have been applied to ensure the safe operation of learning-based locomotion [3, 17]. Hsu et al. [3] introduce a safety monitor based on a value function and fine-tune the corresponding safety filter using a two-stage reinforcement learning framework, providing statistical safety guarantees. However, they consider the uncertainty distribution as a whole, while our work focuses on robustly safeguarding against the worst-case realization of uncertainty. Yang et al. [17] propose a safety monitor criterion based on a heuristically defined safety-triggered set, checking if rollouts activate the criterion. In contrast, our work determines such a safety-triggered set through gameplay rollouts. Additionally, these methods employ a simplified dynamics model and only consider velocity control instead of torque or joint position control directly.

### III. PRELIMINARIES

#### A. Scalable Safety Analysis via Reinforcement Learning

We consider discrete-time, uncertain robot dynamics

$$x_{k+1} = f(x_k, u_k, d_k), \quad (1)$$

where, at each time step  $k \in \mathbb{N}$ ,  $x_k \in \mathcal{X} \subseteq \mathbb{R}^{n_x}$  is the state of the system,  $u_k \in \mathcal{U} \subseteq \mathbb{R}^{n_u}$  is the control input (typically

<sup>2</sup>Some recent efforts have been made to synthesize CBFs based on model predictive methods [16, 28], while the concerned dynamics has no more than 5 state dimensions.

from a control policy  $\pi^u \in \Pi^u: \mathcal{X} \rightarrow \mathcal{U}$ ), and  $d_k \in \mathcal{D} \subseteq \mathbb{R}^{n_d}$  is the disturbance input, unknown *a priori*. The disturbance bound defines the operational design domain (ODD), under which we must ensure autonomous systems function safely and effectively. We further assume we are given a specification of the *failure set*  $\mathcal{F} \subset \mathcal{X}$  of all conditions the system state should never reach. Safety analysis aims to determine the largest possible *safe set*  $\Omega \subset \mathcal{X}$ , from which there exists a control policy that can maintain system safety against all admissible uncertainty realizations (encoded by a disturbance policy  $\pi^d \in \Pi^d: \mathcal{X} \times \mathcal{U} \rightarrow \mathcal{D}$ )

$$\Omega := \{x \in \mathcal{X} \mid \exists \pi^u \in \Pi^u, \forall \pi^d \in \Pi^d, \forall k > 0, x_k \notin \mathcal{F}\}, \quad (2)$$

where  $x_k = \mathbf{x}_x^{\pi^u, \pi^d}(k)$  and  $\mathbf{x}_x^{\pi^u, \pi^d}$  is the system trajectory starting from  $x_0 = x$  and following dynamics (1) with control and disturbance inputs from control policy  $\pi^u$  and disturbance policy  $\pi^d$ , respectively.

Hamilton-Jacobi-Isaacs (HJI) reachability analysis leverages the *level set* representations to transform the binary outcome, or *game-of-kind* as formulated in (2), into a continuous outcome, or *game-of-degree*, by a (Lipschitz-continuous) margin function  $g: \mathcal{X} \rightarrow \mathbb{R}$  such that  $g(x) < 0 \Leftrightarrow x \in \mathcal{F}$  [6, 23]

$$J_k^{\pi^u, \pi^d}(x) := \min_{\tau \in [k, H]} g\left(\mathbf{x}_x^{\pi^u, \pi^d}(\tau)\right), \quad (3)$$

where  $H$  is the concerned control horizon. Consistent with the identifiers in (2), we compute the *lower value* of the game  $V_k(x) := \max_{\pi^u} \min_{\pi^d} J_k^{\pi^u, \pi^d}(x)$ , which gives the disturbance policy information advantage [30]. Additionally, this value function is the fixed-point solution of the Isaacs equation, which can be solved by dynamic programming

$$V_k(x) = \max_u \min_d \min \{g(x), V_{k+1}(f(x, u, d))\}, \quad (4a)$$

$$V_H(x) = g(x). \quad (4b)$$

If a nonempty safe set is present in the context of the differential game, the value function converges and becomes time-independent within this set as  $H \rightarrow \infty$ . Consequently, we can eliminate the dependence on  $k$ , resulting in  $V(x) = \lim_{k \rightarrow \infty} V_k(x)$ . We can recover the (maximal) safe set by the superzero level set of the value function  $\Omega^* = \{x \in \mathcal{X} \mid V(x) \geq 0\}$  and the optimal policies  $\pi^{u^*}, \pi^{d^*}$  from the optimizers of (4).

However, in practice, it is difficult to know the sufficient control horizon *a priori*. Also, finding the maximal safe set is usually difficult to find in complex, high-dimensional dynamics. Instead, *reach-avoid* analysis simplifies the safety analysis by checking whether a control policy exists to guide the system into a (robust controlled-invariant) target set  $\mathcal{T} \subset \mathcal{X}$  ( $\mathcal{T} \cap \mathcal{F} = \emptyset$ ) in  $H$  time steps without entering the failure set previously. The reach-avoid set is defined by

$$\mathcal{RA} := \left\{ x \in \mathcal{X} \mid \exists \pi^u \in \Pi^u, \forall \pi^d \in \Pi^d, \right. \\ \left. \exists k \in [0, H], x_k \in \mathcal{T} \wedge \forall \tau \in [0, k], x_\tau \notin \mathcal{F} \right\}. \quad (5)$$

<sup>3</sup>An example of a margin function is the signed distance function to the failure set.

Since  $\mathcal{T}$  is a robust controlled-invariant set, there exists a policy  $\pi^{\mathcal{T}}$  that can maintain the system state to stay in  $\mathcal{T}$  forever under all disturbance realizations. After the reach-avoid policy safely guides the system into  $\mathcal{T}$ , we can switch to  $\pi^{\mathcal{T}}$  to keep the system in  $\mathcal{T}$  forever. Thus, reach-avoid analysis simplifies the safety control design by requiring only the assurance of control invariance for a small subset of states  $\mathcal{T}$ , which is sufficient for the reach-avoid set to be a safe set.

An auxiliary game of degree can be similarly formulated by introducing another margin function with respect to the target set  $\ell: \mathcal{X} \rightarrow \mathbb{R}$  such that  $\ell(x) \geq 0 \Leftrightarrow x \in \mathcal{T}$ . We consider the reach-avoid outcome [31]

$$J_k^{\pi^u, \pi^d}(x) := \max_{\tau \in [k, H]} \min \left\{ \ell(x_\tau), \min_{s \in [k, \tau]} g(x_s) \right\}. \quad (6)$$

The reach-avoid value function can be solved by the following Isaacs equation

$$V_k(x) = \max_u \min_d \min \{g(x), \max \{\ell(x), V_{k+1}(f(x, u, d))\}\}, \quad (7a)$$

$$V_H(x) = \min \{\ell(x), g(x)\}. \quad (7b)$$

Similarly, the reach-avoid set can be recovered by  $\mathcal{RA} = \{x \in \mathcal{X} \mid V_0(x) \geq 0\}$ .

The computation complexity and memory requirement of solving (4) and (7) grows exponentially with respect to the dimension of continuous states, which limits its applicability to no more than six state dimensions for general dynamics [25]. In recent work, Hsu et al. [29] proposed an adversarial reinforcement learning framework ISAACS to find approximation solutions to the Isaacs equations, where the state-action value function, or Q-function,  $Q_\omega$ , reach-avoid control policy  $\pi_\theta$ , and disturbance policy  $\pi_\psi$  are parameterized by neural networks  $\omega, \theta, \psi$ , respectively.<sup>4</sup> In each iteration of ISAACS, it simulates adversarial safety games to collect state-action sequences, performs gradient updates of neural networks, and determines the policies to sample from in the next simulated games.

### B. Value-Based and Rollout-Based Safety Filters

This section introduces safety filters  $\phi: \mathcal{X} \times \Pi^u \rightarrow \Pi^u$  and  $\phi = (\pi^\bullet, \Delta^\bullet)$ <sup>5</sup> based on switch-type intervention, which can generally be formulated [11]

$$\phi(x, \pi^{\text{task}}) = \begin{cases} \pi^{\text{task}}, & \Delta^\bullet(x, \pi^{\text{task}}) \geq 0, \\ \pi^\bullet, & \text{Otherwise,} \end{cases} \quad (8)$$

where  $\pi^{\text{task}}: \mathcal{X} \rightarrow \mathcal{U}$  is an arbitrary performance-oriented task policy,  $\Delta^\bullet: \mathcal{X} \times \Pi^u \rightarrow \mathbb{R}$ , and  $\pi^\bullet: \mathcal{X} \rightarrow \mathcal{U}$  is a safety-aware or even safety-guaranteed fallback policy.  $\Delta^\bullet$  is a safety monitor if it satisfies that its positive output indicates that the input policy can keep the system safe from the input state.

<sup>4</sup>In reinforcement learning literature,  $Q_\omega$  is also called *critic* as it evaluates the quality of the action, while  $\pi_\theta, \pi_\psi$  are called *actors* since they determine which action to take.

<sup>5</sup>With a slight abuse of notation, we highlight here the safety filter is composed of a safety fallback policy and a safety monitor.

Therefore, the safety filter in (8) maintains the system's safety, following the Theorem 1 in [11]. Our approach introduces a more general and novel safety filter and monitor, considering the task policy as a function rather than just a singular proposed task control.

Previous work has used neural-network-parameterized Q-function for safety monitor with a threshold  $\epsilon > 0$  [3, 32]

$$\Delta_\epsilon^{\bullet, \text{critic}}(x, \pi^{\text{task}}) := Q_\omega(x, \pi^{\text{task}}(x)) - \epsilon. \quad (9)$$

Also, the safety fallback policy can be constructed by  $\text{argmax}_{u \in \mathcal{U}} Q_\omega(x, u)$  or directly  $\pi_\theta$  when the state is outside of the target set. On the other hand, when the state is in the target set  $\mathcal{T}$ ,  $\pi^{\mathcal{T}}$  serves as a fallback to keep the state inside the target set. In other words, the safety fallback policy  $\pi^\bullet$  is defined by a switching rule

$$\pi^\bullet(x) = \begin{cases} \pi^{\mathcal{T}}(x), & x \in \mathcal{T}, \\ \pi_\theta(x), & x \notin \mathcal{T}. \end{cases} \quad (10)$$

Although this *critic filter* has shown practical utility, it does not readily provide safety guarantees. In addition, the value threshold  $\epsilon$  needs to be carefully tuned, which may be difficult for safety-critical applications.

In contrast, the safety monitor can be built on model predictive rollouts. Bastani [33] assumes the dynamical model is perfectly accurate (disturbance-free) and checks if, after executing performance-oriented control, rollout based on the fallback policy satisfies the reach-avoid criterion

$$\Delta_{H, \mathcal{RA}}^{\bullet, \text{nom}}(x, \pi^{\text{task}}) := \mathbb{1} \left\{ \exists \tau \in \{1, \dots, H\}, \hat{x}_\tau \in \mathcal{T} \wedge \forall s \in \{1, \dots, \tau\}, \hat{x}_s \notin \mathcal{F} \right\} - \frac{1}{2} \quad (11)$$

with  $\hat{x}_0 = x$ ,  $\hat{x}_1 = f(x, \pi^{\text{task}}(x), 0)$ , and  $\hat{x}_{\tau+1} = f(\hat{x}_\tau, \pi^\bullet(\hat{x}_\tau), 0)$ ,  $\tau \geq 1$ . Hsu et al. [29] tackle the model mismatch by employing robust rollout with FRS

$$\Delta_{H, \mathcal{RA}}^{\bullet, \text{FRS}}(x, \pi^{\text{task}}) := \mathbb{1} \left\{ \exists \tau \in \{1, \dots, H\}, \mathcal{R}_\tau \subseteq \mathcal{T} \wedge \forall s \in \{1, \dots, \tau\}, \mathcal{R}_s \cap \mathcal{F} = \emptyset \right\} - \frac{1}{2} \quad (12)$$

with  $\mathcal{R}_0 = \{x\}$ ,  $\mathcal{R}_1 = \{f(x, \pi^{\text{task}}(x), d), d \in \mathcal{D}\}$ , and  $\mathcal{R}_{\tau+1} = \{f(\hat{x}, \pi^\bullet(\hat{x}), d), \hat{x} \in \mathcal{R}_\tau, d \in \mathcal{D}\}$ ,  $\tau \geq 1$ . In this work, we instead rely on rollouts of the learned reach-avoid control and disturbance actors to assess system safety risk.

## IV. SAFE WALKING BY ADVERSARIAL GAMEPLAY

This section introduces a systematic way to construct a safety filter for nonlinear, high-dimensional dynamics. In this paper, we specifically consider the task of quadruped walking, but we stress that the method presented is general for different robots and tasks. We start with careful problem formulation by defining state space, control space, uncertainty modeling, and safety specifications. Then, we elucidate offline gameplay learning, where a disturbance actor is jointly trained with the reach-avoid control actor to generate the worst-case realization of uncertainty to attack the system adversarially. We close

the section by systematically constructing an online gameplay filter using the trained control and disturbance policies synthesized from offline learning.

### A. State and Action Spaces

The robot’s state and control input are defined by

$$x = [\mathbf{p}, \dot{\mathbf{p}}, \boldsymbol{\theta}, \dot{\boldsymbol{\theta}}, \boldsymbol{\theta}_J, \dot{\boldsymbol{\theta}}_J], \quad (13a)$$

$$u = [\boldsymbol{\delta}\boldsymbol{\theta}_J] \quad (13b)$$

with  $\mathbf{p}, \boldsymbol{\theta}$  the robot pose,  $\boldsymbol{\theta}_J$  the angular joint position,  $(\dot{\cdot})$  the rate of these variables and  $\boldsymbol{\delta}\boldsymbol{\theta}_J$  the commanded angular increment of the robot’s joint. Appendix A illustrates the state and action space details. Since the robot has three joints per leg, we end up with a 36-D state space and a 12-D control space.

We model the sim-to-real gap via a 6-D adversarial force pushing or pulling the robot with a magnitude of 50 N

$$d = [F_x, F_y, F_z, p_x^F, p_y^F, p_z^F] \quad (13c)$$

with  $F = [F_x, F_y, F_z]$  represents the force vector applied at position defined by  $p_x^F, p_y^F, p_z^F$  in the body coordinates,  $p_x^F, p_y^F \in [-0.1, 0.1]$  m,  $p_z^F \in [0, 0.05]$  m. We further assume the optimal force is bang-bang with  $\|F\|_2 = 50$  N. The red arrows in the imagined gameplay of Fig. 2 show examples of learned adversarial disturbance.

### B. Safety Specifications

We consider the failure set of states where the defined critical points (of the robot’s body)  $\mathbf{p}_g$  are very close to the ground. The safety margin function is defined as

$$g(x) = \min_i \{p_g^i - \bar{p}_g^i\},$$

with  $(\bar{\cdot})$  denotes the desired magnitude.

Also, we consider the target set of states where the concerned variables  $\mathbf{p}_\ell$  are within a small box around the target pose and velocity. The target set is designed so that the robot is known to be robustly stable with a simple stance controller. The target margin function is then defined as

$$\ell(x) = \min_i \{\bar{p}_\ell^i - |p_\ell^i|\}.$$

Appendix A illustrates the safety specifications details.

### C. Offline Gameplay Learning

We introduce an offline gameplay learning scheme, which builds upon ISAACS [29]. At each iteration, the learning algorithm collects interactions with environments via simulated adversarial safety games, updates neural-network-parameterized Q-function and policies, and determines which control and disturbance policies are used for the next iteration’s simulated gameplay.

**Simulated Adversarial Safety Games.** At every time step of games, we store the transition  $(x, u, d, x', \ell', g')$  in the replay buffer  $\mathcal{B}$ , with  $x' = f(x, u, d)$ ,  $\ell' = \ell(x')$  and  $g' = g(x')$ . The control and disturbance inputs are selected

from the policies either trained concurrently or fixed after pre-training.

**Policy and Critic Networks Update** The core of the proposed offline gameplay learning is to find approximate solutions to the Isaacs equation (7). We employ the Soft Actor-Critic (SAC) [34] framework to update the critic and actor networks with the following loss functions. We update the critic to reduce the deviation from the Isaacs target<sup>6</sup>

$$L(\omega) := \mathbb{E}_{(x,u,d,x',\ell',g') \sim \mathcal{B}} \left[ (Q_\omega(x, u, d) - y)^2 \right],$$

$$y = \gamma \min \{ g', \max \{ \ell', Q_{\omega'}(x', u', d') \} \} + (1 - \gamma) \min \{ \ell', g' \} \quad (14a)$$

with  $u' \sim \pi_\theta(\cdot | x')$ ,  $d' \sim \pi_\psi(\cdot | x')$ . We update control and disturbance policies following the policy gradient induced by the critic and entropy loss:

$$L(\theta) := \mathbb{E}_{(x,d) \sim \mathcal{B}} \left[ -Q_\omega(x, \tilde{u}, d) + \alpha^u \log \pi_\theta(\tilde{u} | x) \right], \quad (14b)$$

$$L(\psi) := \mathbb{E}_{(x,u) \sim \mathcal{B}} \left[ Q_\omega(x, u, \tilde{d}) + \alpha^d \log \pi_\psi(\tilde{d} | x) \right], \quad (14c)$$

where  $\tilde{u} \sim \pi_\theta(\cdot | x)$ ,  $\tilde{d} \sim \pi_\psi(\cdot | x)$ , and  $\alpha^u, \alpha^d$  are hyperparameters encouraging higher entropy in the stochastic policies for more exploration, which decay gradually in magnitude through the training.

We can directly train the critic and control and disturbance actors from scratch through (14). On the other hand, we can also utilize a three-level training curriculum with two additional pre-training stages (L1 and L2). In L1, we only train the reach-avoid control actor without considering adversarial disturbance inputs, which is a special case of (14) when  $d = 0$ . Then, in L2, we fix the control policy trained in L1 and train the disturbance policy instead. Since there is only one policy to optimize in L1 and L2, we can use standard SAC directly. At the beginning of the gameplay learning (L3), we can then initialize actor and critic networks with pre-trained weights, i.e., the control actor (L1), disturbance actor (L2), and the safety critic (L2).

Furthermore, L2 training can be viewed as finding the best adversary to attack the *associated* control policies, or simply *best response*  $\pi_\psi^*(\pi^u)$ . After ISAACS training, we additionally use L2 training to fine-tune  $\pi_\psi$  against *frozen*  $\pi_\theta$ . We combine the resulting  $\pi_\psi^*(\pi_\theta)$  into our gameplay filter. On the other hand, we utilize L2 training to perform a bespoke ultimate stress test (BUST) for safety policies and safety filters under various design choices in Table III.

**Policy Selection.** During the L3 training, we also maintain a finite leaderboard of control and disturbance actors from past iterations of training. Periodically, the leaderboard is updated by performing simulated gameplays between the current control and disturbance policies and the previous leaders. If the capacity of the leaderboard is reached, we remove the control

<sup>6</sup>Deep reinforcement learning typically involves training an auxiliary target critic  $Q_{\omega'}$ , with parameters  $\omega'$  that undergo slow adjustments to align with the critic parameters  $\omega$ . This process aims to stabilize the regression by maintaining a fixed target within a relatively short timeframe.

actor checkpoints with the lowest safe rate (and the disturbance actor checkpoints with the highest safe rate). At the next iteration’s simulated adversarial safety games, we randomly select control and disturbance actors from the leaderboard to generate action inputs, which prevents the control actor updates from excessively fitting into a single disturbance actor [35].

#### D. Online Gameplay Safety Filter

This section demonstrates how the reach–avoid control actor  $\pi_\theta$  and disturbance actor  $\pi_\psi$  synthesized offline through game-theoretic reinforcement learning can be systematically used at runtime to construct highly effective safety filters for general nonlinear, high-dimensional dynamic systems. A predictive (rollout-based) safety monitor is employed to prevent tuning the value threshold as the value-based safety monitor, which is difficult to perform before deployment. Also, a simple switching intervention scheme in the form of (8) is used, although optimization-based schemes like CBF–QP are also possible..

The state-of-the-art predictive safety monitors face scalability and robustness challenges. For example, the nominal rollout in (11) can result in an overly optimistic filter, while the FRS-based robust rollout in (12) can be computationally intensive for high-dimensional dynamics. To tackle these challenges, we propose using a novel adversarial gameplay rollout between the fallback and disturbance policy from offline gameplay learning.

The adversarial gameplay begins with applying a control from task policy  $\pi^{\text{task}}$  and fallback policy  $\pi^\bullet$  afterward, with the whole rollout under attacks from the ISAACS disturbance policy  $\pi_\psi$ . This gameplay monitor returns success if the state trajectory safely reaches the target set:

$$\Delta_{H,\mathcal{R},\mathcal{A}}^{\bullet,\text{game}}(x, \pi^{\text{task}}) := \mathbb{1} \left\{ \exists \tau \in \{1, \dots, H\}, \hat{x}_\tau \in \mathcal{T} \wedge \forall s \in \{1, \dots, \tau\}, \hat{x}_s \notin \mathcal{F} \right\} - \frac{1}{2} \quad (15a)$$

with  $\hat{x}_0 = x$ ,  $\hat{x}_{\tau+1} = f(\hat{x}_\tau, \hat{u}_\tau, \pi_\psi(\hat{x}_\tau))$ ,  $\tau \geq 0$ , and

$$\hat{u}_\tau = \begin{cases} \pi^{\text{task}}(\hat{x}_\tau), & \tau = 0, \\ \pi^\bullet(\hat{x}_\tau), & \tau \in \{1, \dots, H-1\}. \end{cases} \quad (15b)$$

Finally, the (real-time) gameplay filter  $\phi = (\pi^\bullet, \Delta^\bullet)$  is constructed by the fallback policy  $\pi^\bullet$  in (10), the gameplay monitor  $\Delta_{H,\mathcal{R},\mathcal{A}}^{\bullet,\text{game}}$  in (15), and a switch-type intervention scheme in (8). Algorithm 1 illustrates the proposed gameplay filter, and Appendix Section A summarizes the terminology (and the symbols) of the modules in safety filters.

However, the computation time in the gameplay rollout may require multiple time steps. To resolve this latency issue, we verify the task policy by a longer execution horizon of  $L$  steps instead of within one step, as in Algorithm 1. The longer foresight also smoothens out undesired oscillations close to the

---

#### Algorithm 1 Real-Time Gameplay Safety Filter

---

**Require:**  $x_k, \pi^{\text{task}}, \pi^\bullet, \pi_\psi, f, L, H$

- 1:  $\hat{x}_0 \leftarrow x_k$
- 2: **for**  $\tau = 0$  to  $H$  **do**
- 3:   **if**  $\tau = 0$  **then**
- 4:      $\pi^u \leftarrow \pi^{\text{task}}$  ▷ Evaluate the task policy
- 5:   **else**
- 6:      $\pi^u \leftarrow \pi^\bullet$  ▷ Followed by the fallback
- 7:      $\hat{u}_\tau \leftarrow \pi^u(\hat{x}_\tau)$
- 8:      $\hat{d}_\tau \leftarrow \pi_\psi(\hat{x}_\tau)$
- 9:      $\hat{x}_{\tau+1} \leftarrow f(\hat{x}_\tau, \hat{u}_\tau, \hat{d}_\tau)$
- 10:    **if**  $g(\hat{x}_{\tau+1}) < 0$  **then** ▷ Gameplay violates safety
- 11:      $\text{res} \leftarrow 0$
- 12:     **return**  $\text{res}, \pi^\bullet$
- 13:    **if**  $\ell(\hat{x}_{\tau+1}) > 0$  **then** ▷ Gameplay succeeds
- 14:      $\text{res} \leftarrow 1$
- 15:    **return**  $\text{res}, \pi^{\text{task}}$
- 16:  $\text{res} \leftarrow 0$  ▷ Gameplay does not reach
- 17: **return**  $\text{res}, \pi^\bullet$

---

boundary of the reach–avoid set. The gameplay-based safety monitor with latency is formulated below

$$\Delta_{H,L,\mathcal{R},\mathcal{A}}^{\bullet,\text{game}}(x, \pi^{\text{task}}) := \mathbb{1} \left\{ \exists \tau \in \{2L, \dots, H\}, \hat{x}_\tau \in \mathcal{T} \wedge \forall s \in \{L, \dots, \tau\}, \hat{x}_s \notin \mathcal{F} \right\} - \frac{1}{2} \quad (16a)$$

with  $\hat{x}_0 = x$ ,  $\hat{x}_{\tau+1} = f(\hat{x}_\tau, \hat{u}_\tau, \pi_\psi(\hat{x}_\tau))$ ,  $\tau \geq 0$ , and

$$\hat{u}_\tau = \begin{cases} \phi^{\text{prev}}(\hat{x}_\tau), & \tau \in \{0, \dots, L-1\}, \\ \pi^{\text{task}}(\hat{x}_\tau), & \tau \in \{L, \dots, 2L-1\}, \\ \pi^\bullet(\hat{x}_\tau), & \tau \in \{2L, \dots, H-1\}, \end{cases} \quad (16b)$$

where  $\phi^{\text{prev}}$  is the verified gameplay filter and is executed, and thus immutable, during the wait for simulated adversarial gameplay. In other words, if the (trained) disturbance policy captures the worst-case realization of the uncertainty and sim-to-real gap, executing  $\phi^{\text{prev}}$  is guaranteed safe. However, we may not have the optimal disturbance policy due to the parameterization of neural networks. Instead, we still switch to the fallback  $\pi^\bullet$  if there is a safety failure during the first  $L$  steps in the imagined gameplay. Algorithm 2 summarizes the  $L$ -step gameplay safety filter.

Fig. 2 illustrates the operation of the gameplay safety filter with the  $L$ -step gameplay safety monitor. For example, at monitor cycle  $k = L$ , since the safety monitor check is successful at  $k = 0$ ,  $\phi^{\text{prev}} = \pi^{\text{task}}$ . On the other hand, at monitor cycle  $k = 2L$ , since the safety monitor check is failed at  $k = L$ ,  $\phi^{\text{prev}} = \pi^\bullet$ .

## V. EXPERIMENTS

Through extensive simulation study and hardware experiments, we aim to answer the following questions: Can our offline game-theoretic learning and gameplay safety filter

- (1) achieve robust safety for general nonlinear, high-dimensional systems without obstructing task execution?

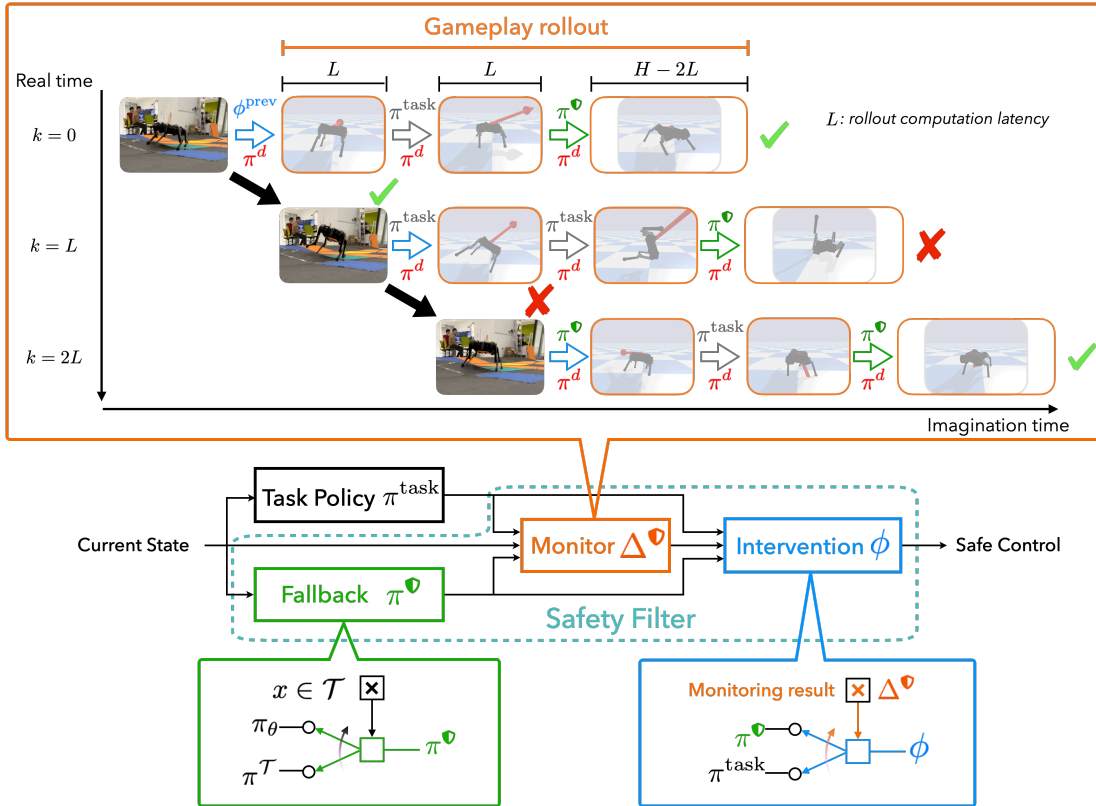


Fig. 2: **The operation of the gameplay safety filter.** *Top:* The  $L$ -step gameplay monitor evaluates  $\pi^{\text{task}}$  for  $L$  steps. Since the gameplay result is successful at time step 0, the safety filter executes task policy from  $L$  to  $2L - 1$  steps. On the other hand, the safety filter employs  $\pi^{\text{v}}$  from  $2L$  to  $3L - 1$  steps due to the failure result of gameplay imagination at time step  $L$ . *Middle:* The block diagram of safety filters shows they are modular to any  $\pi^{\text{task}}$ . *Bottom:* The safety fallback policy alternates between  $\pi^{\text{T}}$  and  $\pi_{\theta}$ , while the safety filter employs a switch-type intervention between  $\pi^{\text{task}}$  and  $\pi^{\text{v}}$  given the safety monitor’s result.

- (2) enable the robot to operate safely in various deployment conditions that are different from the training conditions in a “zero-shot” manner?
- (3) outperform reward-based learning, non-game-theoretic learning, and value-based (critic) safety filters?

Additionally, we analyze the relative importance of our design choices, including (a) gameplay filter with reach-avoid criteria versus avoid-only, (b) three-level training curriculum versus L3 directly, and (c) symmetric exploitation in offline learning versus without.

#### A. Experiment Setup

**Robot and sensors.** We use Spirit 40 from Ghost Robotics for the robot platform as shown in Fig. 1 and the PyBullet physics engine [36] to construct the simulated environment. We use the internal motor encoder of the robot to obtain joint absolute position  $\theta_j^i$  and velocity  $\omega_j^i$ , and built-in IMU for roll  $\theta_x$  and pitch  $\theta_y$ , body axial rotational rate  $\omega_x, \omega_y, \omega_z$  and velocity  $v_x, v_y, v_z$ . There is no force sensor or contact sensing capability enabled, meaning that ground contact can only be implicitly inferred.

**Gameplay filter.** To implement a gameplay safety filter on a physical robot, we create a gameplay rollout server, a

ROS service that takes in the current physical robot state and proposed control action. The server then runs the gameplay rollout for a fixed horizon and returns the filtered safe action. Using the reach-avoid criterion for the gameplay rollout terminal condition, we observe a flat change in elapsed time (from request to response) when the rollout horizon increases (from 10 to 300 steps), yielding an average cycle of 35 Hz.

**Task and perturbations.** We construct two different terrains for physical experiments: flat terrain with tugging forces and unmodeled irregular terrain. The robot’s task is to traverse safely across from the same state initialization to reach the goal on the other side of the terrain.

To emulate adversarial tugging forces on the robot, we mount a rope to the robot on one end and a motion-tracked dynamometer on the other end to monitor the force magnitude and direction. The dynamometer has a rated capacity of 500 N and a resolution of 0.1 N, tethered to a computer via RS232C. The sampling rate is 1000 Hz to record both constant pulling and force pulses.

The irregular terrain is a  $2 \text{ m} \times 4 \text{ m}$  area with a 15-degree incline along one edge, and two mounds emerged in the middle using memory foam, with length  $\times$  width  $\times$  height of  $1.2 \text{ m} \times 0.7 \text{ m} \times 0.05 \text{ m}$  and  $1.2 \text{ m} \times 0.8 \text{ m} \times 0.15 \text{ m}$ , positioned 1.8 m

---

**Algorithm 2** *L*-Step Gameplay Safety Filter

---

**Require:**  $x_k, \pi^{\text{task}}, \phi^{\text{prev}}, \pi^{\mathbf{V}}, \pi_\psi, f, L, H$

```

1:  $\hat{x}_0 \leftarrow x_k$ 
2: for do
3:
4:
5:
6: for  $\tau=0$  to  $H$  do
7:   if  $\tau < L$  then
8:      $\pi^u \leftarrow \phi^{\text{prev}}$            ▷ Apply the verified filter
9:   else if  $\tau < 2L$  then
10:     $\pi^u \leftarrow \pi^{\text{task}}$        ▷ Evaluate the task policy
11:   else
12:     $\pi^u \leftarrow \pi^{\mathbf{V}}$          ▷ Followed by the fallback
13:     $\hat{u}_\tau \leftarrow \pi^u(\hat{x}_\tau)$ 
14:     $\hat{d}_\tau \leftarrow \pi_\psi(\hat{x}_\tau)$ 
15:     $\hat{x}_{\tau+1} \leftarrow f(\hat{x}_\tau, \hat{u}_\tau, \hat{d}_\tau)$ 
16:    if  $g(\hat{x}_{\tau+1}) < 0$  then   ▷ Gameplay violates safety
17:       $\text{res} \leftarrow 0$ 
18:    return  $\text{res}, \pi^{\mathbf{V}}$ 
19:    if  $\ell(\hat{x}_{\tau+1}) > 0$  and  $\tau \geq 2L$  then   ▷ Gameplay
succeeds
20:       $\text{res} \leftarrow 1$ 
21:    return  $\text{res}, \pi^{\text{task}}$ 
 $\text{res} \leftarrow 0$            ▷ Gameplay does not reach
22: return  $\text{res}, \pi^{\mathbf{V}}$ 

```

---

away from each other.

**Baselines.** To evaluate the effectiveness of margin-based feedback signal and uncertainty-aware offline learning, we consider three prior reinforcement learning algorithms: (1) standard SAC [34] with reward defined as

$$r(x) = \begin{cases} 1, & x \in \mathcal{T}, \\ -1, & x \in \mathcal{F}, \\ 0, & \text{Otherwise,} \end{cases}$$

(2) non-game-theoretic reach-avoid reinforcement learning (RARL) [31], RARL with the domain randomization (DR), and (4) adversarial SAC with the reward feedback signal. For the critic filter, we conduct a parameter sweep to find the best value threshold in the simulation and use the same threshold in physical experiments directly.

**Policy.** We handcraft a task policy by using an inverse kinematics gait planner for forward walking and sideways walking. We parameterize all policies by neural networks of 3 fully connected layers with 256 neurons, and critics have 3 layers with 128 neurons. The gameplay filter uses horizon  $H = 300$  and  $L = 1$ . We use a low-level PD position controller that outputs torques  $\tau^i = K_p(\delta\theta_j^i) - K_d \cdot \omega_j^i$  to the robot motor controller with  $K_p, K_d$  the proportional and derivative gains.

## B. Physical Results

**Safe walking on different terrains.** We answer Questions (1) and (3) by evaluating physical robots walking on flat terrain with tugging force and bumpy terrain. We compare our proposed gameplay safety filter with the task policy and critic safety filter. We record the number of runs that the quadruped can safely reach the goal. Also, for those successful runs, we also report the frequency of filter intervention and the time to reach the goal. We additionally report the maximum and average (adversarial) force in the walk for the experiment of flat terrain with tugging forces. Table I shows the result of the experiment.<sup>7</sup> Our proposed gameplay safety filter has the highest safe rate on both flat terrain with tugging force and unmodeled irregular terrain. Even for those failed trials, the gameplay filter withstands higher tugging force before it violates the safety constraints. Further, the gameplay filter does not unduly intervene with the task-oriented actions as it has a similar filter frequency as the critic filter.

Fig. 1 shows the quadruped walking by applying the proposed gameplay filter versus the performance-oriented task policy. When there are imminent safety failures after executing candidate performance-oriented controls, e.g., with airborne legs or loss of balance when climbing, the gameplay filter intervenes and stretches the legs of the quadruped to fight against persistent forces and bumpy terrain.

**Maximum withstandable force.** To answer Question (3), we test the maximum tugging force withstandable for the safety policies trained by ISAACS, SAC with reward, reach-avoid reinforcement learning with domain randomization (RARL+DR), and adversarial SAC with reward. We pull the quadruped from different directions, where the tugging angle for “low” is always between  $[-0.1, 0.4]$  rad, and the tugging angle for “high” is always between  $[0.5, 1.0]$  rad.

Table II shows that the employed  $\pi_\theta$  can withstand more than about 150 N from all directions, but the non-game-theoretic counterpart (RARL+DR) is vulnerable to the tugging from the left and can only withstand 43 N. This observation suggests that DR struggles to capture the worst-case realization of disturbances accurately. This limitation arises from the inherent nature of DR, where the control actor is optimized for average disturbance behavior. As the dimension of disturbance input increases, the likelihood of the random policy simulating the worst-case disturbance decreases exponentially. This underscores the importance of employing adversarial game-theoretic learning techniques over DR approaches.

Further, we notice the reward-based reinforcement learning baselines and ISAACS with the avoid-only objective fail almost immediately before applying the force since they overreact and thus flip the robot. We find that reach-avoid policies generalize better since they can bring the robot to a stable stance. We also include tests for task policy  $\pi^{\text{task}}$  and the fixed-pose policy  $\pi^{\mathcal{T}}$  (used when the state is in the target

<sup>7</sup>There is one test of critic safety filter on bumpy terrains failing to reach the goal but remaining safe. We do not include this run’s filter frequency and elapsed time for the average.

TABLE I: We evaluate physical robots walking on flat terrain with tugging force and unmodeled irregular terrain.  $F_{\text{avg}}$  and  $F_{\text{max}}$  are the average and maximum force during the test and  $T_{\text{goal}}$  is the time to reach the goal. Our gameplay filter has the highest safe rate in both tugging force and irregular terrain tests without overly intervening in task-oriented actions.

Policy	Tugging Force						Bumpy Terrain			
	Safe Rate	Successful Runs				Failed Runs		Safe Rate	Successful Runs	
		Filter Freq.	$T_{\text{goal}}$	$F_{\text{avg}}^{\text{peak}}$	$F_{\text{max}}^{\text{peak}}$	$F_{\text{avg}}^{\text{peak}}$	$F_{\text{min}}^{\text{peak}}$		Filter Freq.	$T_{\text{goal}}$
$\phi^{\text{game}}$	7/10	0.17	26.3	67.5N	70.5N	59.8N	52.7N	10/10	0.19	41.2
$\phi^{\text{critic}}$	4/10	0.10	26.8	73.7N	80.9N	53.6N	40.0N	5/10	0.22	33.5
$\pi^{\text{task}}$	0/10	n/a	n/a	n/a	n/a	56.5N	41.4N	5/10	n/a	16.4

TABLE II: Maximum force magnitude withstood by the physical robot with various safety policies<sup>†</sup>, task policy  $\pi^{\text{task}}$ , and fixed-pose policy  $\pi^{\mathcal{T}}$  in different tugging directions. Our employed fallback  $\pi^{\heartsuit}$  outperforms the task policy and other safety fallback baselines and has comparable robustness to the policy used in the target set.

Algorithm	Maximum Force			
	Left		Right	
	Low	High	Low	High
$\pi^{\heartsuit}$	87.1N*	61.1N*	99.3N*	59.1N*
$\pi_{\theta}$	100.5N*	150.3N*	121.6N*	121.9N*
RARL + DR	46.4N	43N	57.2N	72.1N*
$\pi^{\text{task}}$	83.2N	96.9N	82.8N*	59N
$\pi^{\mathcal{T}}$	151.9N*	173.7N*	140.3N*	142.6N*

<sup>†</sup> Safety policies from reward-based reinforcement learning and ISAACS with the avoid-only objective fail immediately before applying force.

\* The policy can withstand this magnitude of force. Since the policy can make the quadruped move toward the tugging direction, we cannot add more force in 10 pull attempts.

set). We observe that ISAACS control actor is strictly better than  $\pi^{\text{task}}$  and is comparable to  $\pi^{\mathcal{T}}$ .

### C. Simulated Results

**Bespoke ultimate stress test (BUST).** We further answer Questions (1) and (3) by running more exhaustive case studies comparing the following policies: task policy  $\pi^{\text{task}}$ , ISAACS control actor  $\pi_{\theta}$ , critic safety filter  $\phi^{\text{critic}}$ , and proposed gameplay safety filter  $\phi^{\text{game}}$ . In order to test their robustness when taken to the limit, we learn, for each of the above control schemes, a *specialized* adversarial disturbance policy explicitly trained (via L2) to exploit its safety vulnerabilities. We also compare these policies against random perturbations sampled uniformly from the disturbance set  $\pi^{\text{rnd}}$  or from extreme points (e.g.,  $F_x = 50, F_y = F_z = 0$ )  $\pi^{\text{rnd},+}$ .

In L2 training, the disturbance actor must face a time-independent optimal control problem, where the control policy (including the appropriate safety filter) is queried during environment simulation. We note that while the internally *simulated* gameplay rollout considers a time-varying policy, the *executed* safety-filtered policy  $\phi^{\text{game}}$  remains time-independent. Specifically,  $\phi^{\text{game}}$  selects either the task control or the safety fallback control based on the outcome of the gameplay rollout, with the rollout dependent solely on the initial state but not *when* this state is visited. Therefore,  $\phi^{\text{game}}$

can be considered part of the time-invariant environment, meeting the requirements of L2 training.

Table III shows the result of the BUST. We first note that  $\pi^{\text{task}}$  is vulnerable to all  $\pi_{\psi}^*$ , while the proposed gameplay filters can only be exploited by its associated  $\pi_{\psi}^*(\phi^{\text{game}})$ . Further, because  $\phi^{\text{game}}$  is very robust, this helps  $\pi_{\psi}^*(\phi^{\text{game}})$  attack effectively against other policies, where the third column has the lowest safe rates compared to other columns.

The last 2 columns show the safe rate under random disturbance. Except for  $\pi^{\text{task}}$ , both the reach-avoid control actor and safety filters remain at high safe rates. This observation suggests that our L2 training method effectively establishes a superior safety benchmark for policies compared to DR, even when we improve the sampling from uniformly within the set  $\pi^{\text{md}}$  to extreme cases  $\pi^{\text{md},+}$ .

#### Sensitivity analysis: reach-avoid criteria vs. avoid-only.

We evaluate the significance of using reach-avoid criteria in the gameplay filter by performing a sensitivity analysis of the horizon in the imagined gameplay. Fig. 3 shows that the gameplay filter with reach-avoid criteria still remains 100% safe rate even when the gameplay horizon is short ( $H = 10$ ). However, the gameplay filter with avoid-only criteria, which simplifies (16a)

$$\Delta_{H,L,A}^{\heartsuit,\text{game}}(x, \pi^{\text{task}}) := \mathbb{1}\{\forall \tau \in \{L, \dots, H\}, \hat{x}_{\tau} \notin \mathcal{F}\} - \frac{1}{2}, \quad (17)$$

has more safety violations than task policy when  $H = 10$ . The difference is due to shorter imagined gameplay resulting in more frequent filter intervention for reach-avoid criteria but overly optimistic monitoring for avoid-only criteria (ignore the upcoming failure). Further, as the gameplay horizon increases, the filter frequency of using reach-avoid criteria goes down, i.e., if  $H \geq H'$

$$\Delta_{H,L,\mathcal{R},A}^{\heartsuit,\text{game}} < 0 \rightarrow \Delta_{H',L,\mathcal{R},A}^{\heartsuit,\text{game}} < 0. \quad (18)$$

This observation indicates that reach-avoid criteria are preferred in physical deployment as it is difficult to know the sufficient horizon *a priori*.

**Sensitivity analysis: three-level training curriculum.** We testify to the need to use a three-level curriculum by gameplay results against a specialized adversary for the reach-avoid control actor trained with the curriculum, i.e.,  $\pi_{\psi}^*(\pi_{\theta})$ . Fig. 4 shows the safe rate of gameplay results between the model checkpoints stored along the training and  $\pi_{\psi}^*(\pi_{\theta})$ . We observe

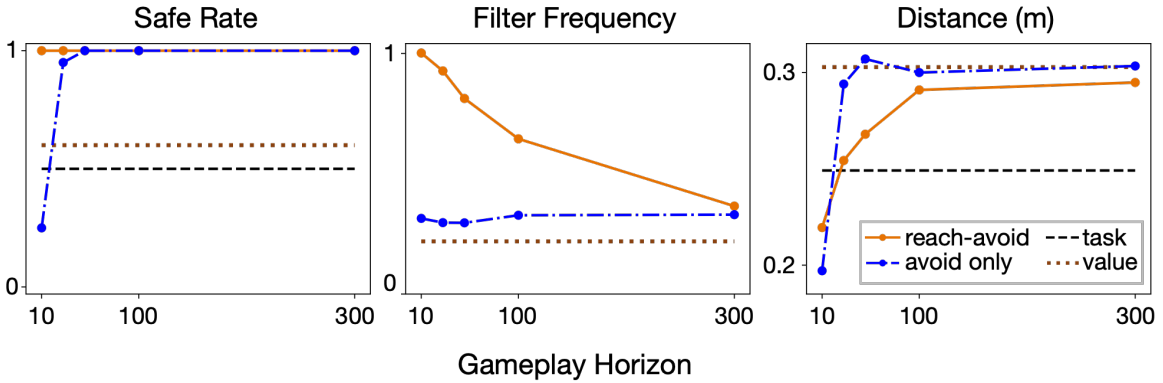


Fig. 3: Sensitivity analysis of gameplay horizon and gameplay criteria. The proposed gameplay safety filter, utilizing the reach-avoid criteria, maintains a 100% safe rate for all gameplay horizons. As the gameplay horizon shortens, the gameplay filter with reach-avoid criteria only experiences a decrease in filter efficiency without compromising safety. In contrast, the filter with avoid-only criteria shows more safety violations than the task policy under a very short horizon. Also, our proposed gameplay filter shows a higher safe rate than the critic safety filter and task policy.

TABLE III: We perform a bespoke ultimate stress test in simulated environments by learning a *specialized* adversarial disturbance policy explicitly trained (via L2) to exploit any existing vulnerabilities in each of these robot controllers  $\pi_\theta$ ,  $\pi^{\text{task}}$ ,  $\phi^{\text{game}}$ ,  $\phi^{\text{critic}}$ . Additionally, we consider random disturbance sampled uniformly in all directions  $\pi^{\text{rnd}}$  or at extreme directions  $\pi^{\text{rnd},+}$ . The proposed gameplay filter  $\phi^{\text{game}}$  has a higher safe rate than the task policy  $\pi^{\text{task}}$ , critic filter  $\phi^{\text{critic}}$  and the learned reach-avoid actor  $\pi_\theta$ .

	$\pi_\psi^*(\pi_\theta)$	$\pi_\psi^*(\pi^{\text{task}})$	$\pi_\psi^*(\phi^{\text{game}})$	$\pi_\psi^*(\phi^{\text{critic}})$	$\pi^{\text{rnd}}$	$\pi^{\text{rnd},+}$
$\pi_\theta$	0.37	0.38	0.17	0.44	0.88	0.85
$\pi^{\text{task}}$	0.0	0.0	0.0	0.0	0.03	0.03
$\phi^{\text{game}}$	0.42	0.35	0.03	0.45	0.84	0.89
$\phi^{\text{critic}}$	0.37	0.34	0.10	0.44	0.86	0.86

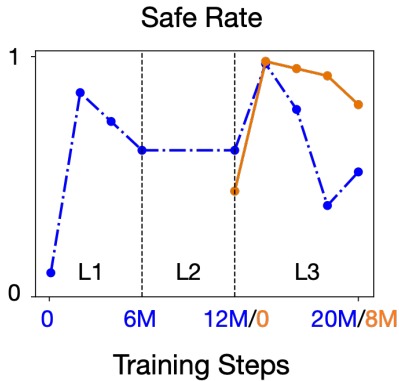


Fig. 4: We evaluate the impact of the three-level curriculum by retrospectively measuring the effectiveness of the *trainee* control actor against the *fully trained* disturbance actor. Contrary to our initial expectation, the two pertaining stages do not present noticeable advantages over direct learning.

that two pre-training stages in the curriculum do not significantly improve training performance. In contrast, directly learning in the L3 stage requires similar steps in gameplay learning to reach a decent safety performance.

## VI. CONCLUSION

This work presents a game-theoretic learning approach to synthesize safety filters for high-order, nonlinear dynamics. The proposed gameplay safety filter monitors the risk of system safety through imagined games between its best-effort safety fallback policy and a learned virtual adversary, aiming to realize the worst-case uncertainty in the system. We validate our approach on a physical quadruped robot under strong tugging forces and unmodeled irregular terrain while maintaining zero-shot safety. An exhaustive simulation study is performed to compare with state-of-the-art safety fallback policies, safety filters, and understand the relative importance of design choices.

### APPENDIX A IMPLEMENTATION DETAILS

The state and action space are defined as:

$$x = [p_x, p_y, p_z, v_x, v_y, v_z, \theta_x, \theta_y, \theta_z, \omega_x, \omega_y, \omega_z, \{\theta_j^i\}, \{\omega_j^i\}],$$

$$u = [\{\delta\theta_j^i\}],$$

with  $p_x, p_y, p_z$  the position of the body center,  $v_x, v_y, v_z$  the velocity of the robot in the body frame coordinate,  $\theta_x, \theta_y, \theta_z$  the roll, pitch, and yaw of the robot,  $\omega_x, \omega_y, \omega_z$  the body axial

TABLE IV: Implementation details of the safety specifications of quadruped walking.

Notation	Magnitude
$\bar{z}_{\text{corner},g}$	0.1 m
$\bar{z}_{\text{knee}}$	0.05 m
$\bar{z}_{\text{corner},\ell}$	0.4 m
$\bar{z}_{\text{toe}}$	0.05 m
$\bar{\omega}$	10 deg/s
$\bar{v}$	0.2 m/s

rotational rate, and  $\theta_j^i, \omega_j^i, \delta\theta_j^i$  the angle, angular velocity, and commanded angular increment of the robot's  $i^{\text{th}}$  joint.<sup>8</sup>

We define the critical points  $\mathbf{p}_c$  as the body corners and knees of the robot. The safety margin is defined as:

$$g(x) = \min \left\{ \min_i \{z_{\text{corner}}^i\} - \bar{z}_{\text{corner},g}, \min_i \{z_{\text{knee}}^i\} - \bar{z}_{\text{knee}} \right\},$$

with  $z_{\text{corner}}^i$  the distance to ground of robot body corner  $i^{\text{th}}$  and  $z_{\text{knee}}^i$  the distance to ground of robot knee  $i^{\text{th}}$ .

The target margin function is defined as

$$\ell(x) = \min \left\{ \bar{\omega} - |\omega_x|, \bar{\omega} - |\omega_y|, \bar{\omega} - |\omega_z|, \bar{v} - |v_x|, \bar{v} - |v_y|, \bar{v} - |v_z|, \bar{z}_{\text{corner},\ell} - \max_i \{z_{\text{corner}}^i\}, \bar{z}_{\text{toe}} - \max_i \{z_{\text{toe}}^i\} \right\},$$

with  $z_{\text{toe}}^i$  the distance to ground of robot toes  $i^{\text{th}}$ .  $(\bar{\cdot})$  denotes the desired magnitude. Table IV shows the threshold used to define the safety and target margin functions for quadruped walking.

Table V summarizes the terminology used in safety filter design, which also highlights the modularity of the proposed gameplay filter.

## APPENDIX B

### SENSITIVITY ANALYSIS: SYMMETRY EXPLOITATION

We notice that in some training runs, the disturbance actor always attacks from a fixed direction (e.g., the positive direction of the y-axis), which results in the reach-avoid control actor being vulnerable to the attack in the other direction (e.g., the negative direction of the y-axis). To prevent this overfitting, we utilize the symmetry in robot locomotion by flipping the disturbance inputs in the collected interactions and re-simulate the new disturbance sequences, i.e.,  $\tilde{d} = [F_x, -F_y, F_z, p_x, p_y, p_z]$ . This data augmentation technique helps with obtaining a symmetric disturbance behavior more quickly and robustifying the control actor.

Fig. 5 shows the Q-function value and the adversarial force in y-direction  $F_y$  from the (trained) disturbance policy under different roll angles while fixing other state variables and zero control signal with and without symmetry exploitation. The Q-function value curve's symmetry with respect to changes in roll angle is improved. The realized worst-case learned adversarial

<sup>8</sup>In this work, we specifically consider walking locomotion, so the policies ignore  $p_x, p_y, p_z, \theta_z$ .

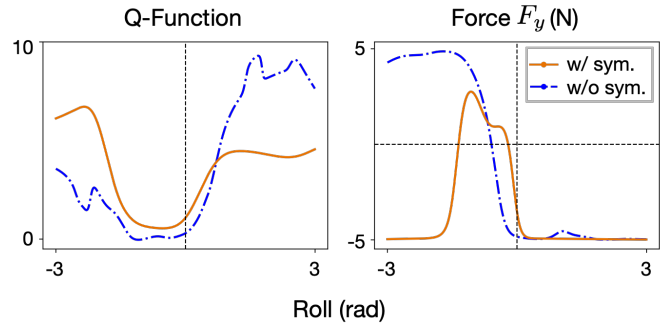


Fig. 5: Effectiveness of symmetry exploitation. Improved symmetry in Q-function values and adversarial forces ( $F_y$ ) indicates a balanced response to disturbances, where exploiting symmetry follows  $F_y < 0$  for positive roll angles and  $F_y > 0$  for negative roll angles.

force also reflects the effectiveness of this exploitation: when the roll angle is positive, an effective way to further worsen the situation is to apply an external force with  $F_y < 0$ , further increasing the roll value, and similarly,  $F_y > 0$  when roll angle is negative. The  $F_y$  curve under exploitation crosses roll=0 axis much earlier. With a better realization of the worst-case disturbance, the sim-to-real gap can be minimized, as learning to counter a balanced disturbance could result in a balanced response.

## REFERENCES

- [1] A. Kumar, Z. Fu, D. Pathak, and J. Malik. “RMA: Rapid Motor Adaptation for Legged Robots”. *Proc. Robotics: Science and Systems*. July 2021.
- [2] Z. Zhuang, Z. Fu, J. Wang, et al. “Robot Parkour Learning”. *Conf. Robot Learning*. Vol. 229. Proceedings of Machine Learning Research. Nov. 2023, pp. 73–92.
- [3] K.-C. Hsu, A. Z. Ren, D. P. Nguyen, A. Majumdar, and J. F. Fisac. “Sim-to-Lab-to-Real: Safe Reinforcement Learning with Shielding and Generalization Guarantees”. *Artificial Intelligence* 314 (2023), p. 103811.
- [4] G. Margolis, G. Yang, K. Paigwar, T. Chen, and P. Agrawal. “Rapid Locomotion via Reinforcement Learning”. *Proc. Robotics: Science and Systems*. New York City, NY, USA, June 2022.
- [5] I. Kostrikov, L. M. Smith, and S. Levine. “Demonstrating A Walk in the Park: Learning to Walk in 20 Minutes With Model-Free Reinforcement Learning”. *Proc. Robotics: Science and Systems*. Daegu, Republic of Korea, July 2023.
- [6] S. Bansal, M. Chen, S. Herbert, and C. J. Tomlin. “Hamilton-Jacobi reachability: A brief overview and recent advances”. *Proc. IEEE Conf. Decision and Control*. 2017, pp. 2242–2253.
- [7] M. Bui, M. Lu, R. Hojabr, M. Chen, and A. Shriraman. “Real-Time Hamilton-Jacobi Reachability Analysis of Autonomous System with an FPGA”. *IEEE/RSJ Int.*

TABLE V: Terminology and symbols used in safety filter modules.

Category	Components	Description
Safety Filter ( $\phi^{\text{critic}}, \phi^{\text{game}}$ )	Safety Fallback Policy ( $\pi^{\mathbf{V}}$ )	The policy to execute when the safety monitor output is negative.
	Safety Monitor ( $\Delta^{\mathbf{V}}$ )	The safety monitor returns a positive value if the input policy can maintain the system’s safety from the input state.
Safety Fallback Policy ( $\pi^{\mathbf{V}}$ )	Reach–Avoid Control Actor ( $\pi_{\theta}$ )	The learned safety fallback when the current state <i>is not</i> in the target set, which guides the system to reach the target set safely.
	Controlled-Invariant Policy ( $\pi^{\mathcal{T}}$ )	The safety fallback when the current state is <i>in</i> the target set, which keeps the system in the target set.
Safety Monitor ( $\Delta_{\epsilon}^{\mathbf{V}, \text{critic}}, \Delta^{\mathbf{V}, \text{game}}$ )	Reach–Avoid Control Actor ( $\pi_{\theta}$ )	The same in the above section.
	Disturbance Actor ( $\pi_{\psi}$ )	The learned disturbance policy that tries to simulate the worst-case uncertainty realization in the ODD to attack the system.
	Critic ( $Q_{\omega}$ )	The learned state-action value function, whose values indicate the minimum separation from the failure set and maximum distance to the target set.
Task Policy ( $\pi^{\text{task}}$ )	Dynamics Model ( $f$ )	The discrete-time, uncertain robot dynamics model used to simulate the imagined gameplay.
	n/a	The policy that cares about the task performance, which can ignore the safety constraints.

- Conf. Intelligent Robots & Systems*. Prague, Czech Republic, Sept. 27, 2021, pp. 1666–1673.
- [8] Q. Nguyen and K. Sreenath. “Robust Safety-Critical Control for Dynamic Robotics”. *IEEE Transactions on Automatic Control* 67.3 (Mar. 2022), pp. 1073–1088.
- [9] T. G. Molnar, R. K. Cosner, A. W. Singletary, W. Ubellacker, and A. D. Ames. “Model-Free Safety-Critical Control for Robotic Systems”. *IEEE Robotics and Automation Letters* 7.2 (Apr. 2022), pp. 944–951.
- [10] E. Collaboration, A. Padalkar, A. Pooley, et al. “Open X-Embodiment: Robotic Learning Datasets and RT-X Models”. 2023.
- [11] K.-C. Hsu, H. Hu, and J. F. Fisac. “The Safety Filter: A Unified View of Safety-Critical Control in Autonomous Systems”. 2023.
- [12] J. F. Fisac, A. K. Akametalu, M. N. Zeilinger, S. Kaynama, J. Gillula, and C. J. Tomlin. “A General Safety Framework for Learning-Based Control in Uncertain Robotic Systems”. *IEEE Transactions Automatic Control* 64.7 (2019), pp. 2737–2752.
- [13] A. D. Ames, X. Xu, J. W. Grizzle, and P. Tabuada. “Control Barrier Function Based Quadratic Programs for Safety Critical Systems”. *IEEE Transactions Automatic Control* 62.8 (2017), pp. 3861–3876.
- [14] K. P. Wabersich and M. N. Zeilinger. “Linear model predictive safety certification for learning-based control”. *Proc. IEEE Conf. Decision and Control*. 2018, pp. 7130–7135.
- [15] O. Bastani and S. Li. “Safe Reinforcement Learning via Statistical Model Predictive Shielding”. *Proc. Robotics: Science and Systems*. July 2021.
- [16] A. Ramesh Kumar, K.-C. Hsu, P. J. Ramadge, and J. F. Fisac. “Fast, Smooth, and Safe: Implicit Control Barrier Functions Through Reach-Avoid Differential Dynamic Programming”. *IEEE Control Systems Letters* 7 (2023), pp. 2994–2999.
- [17] T.-Y. Yang, T. Zhang, L. Luu, S. Ha, J. Tan, and W. Yu. “Safe Reinforcement Learning for Legged Locomotion”. *IEEE/RSJ Int. Conf. Intelligent Robots & Systems*. 2022, pp. 2454–2461.
- [18] G. Bledt, M. J. Powell, B. Katz, J. Di Carlo, P. M. Wensing, and S. Kim. “MIT Cheetah 3: Design and Control of a Robust, Dynamic Quadruped Robot”. *IEEE/RSJ Int. Conf. Intelligent Robots & Systems*. 2018, pp. 2245–2252.
- [19] A. W. Winkler, C. D. Bellicoso, M. Hutter, and J. Buchli. “Gait and Trajectory Optimization for Legged Systems Through Phase-Based End-Effector Parameterization”. *IEEE Robotics and Automation Letters* 3.3 (2018), pp. 1560–1567.
- [20] J. Tobin, R. Fong, A. Ray, J. Schneider, W. Zaremba, and P. Abbeel. “Domain randomization for transferring deep neural networks from simulation to the real world”. *IEEE/RSJ Int. Conf. Intelligent Robots & Systems*. 2017, pp. 23–30.
- [21] A. Z. Ren, H. Dai, B. Burchfiel, and A. Majumdar. “AdaptSim: Task-Driven Simulation Adaptation for Sim-to-Real Transfer”. *Conf. Robot Learning*. Vol. 229. Proceedings of Machine Learning Research. Nov. 2023, pp. 3434–3452.
- [22] F. Ramos, R. Possas, and D. Fox. “BayesSim: Adaptive Domain Randomization Via Probabilistic Inference for Robotics Simulators”. *Proc. Robotics: Science and Systems*. Freiburg/Breisgau, Germany, June 2019.
- [23] I. M. Mitchell. “The flexible, extensible and efficient toolbox of level set methods”. *Journal Scientific Computing* 35.2 (2008), pp. 300–329.

- [24] J. F. Fisac, M. Chen, C. J. Tomlin, and S. S. Sastry. “Reach-Avoid Problems with Time-Varying Dynamics, Targets and Constraints”. *Hybrid Systems: Computation and Control*. Seattle, WA, USA, 2015, pp. 11–20.
- [25] M. Bui, G. Giovanis, M. Chen, and A. Shriraman. “OptimizedDP: An Efficient, User-friendly Library For Optimal Control and Dynamic Programming”. 2022.
- [26] A. D. Ames, S. Coogan, M. Egerstedt, G. Notomista, K. Sreenath, and P. Tabuada. “Control Barrier Functions: Theory and Applications”. *European Control Conference*. 2019, pp. 3420–3431.
- [27] E. D. Sontag. “A Lyapunov-like characterization of asymptotic controllability”. *SIAM journal on control and optimization* 21.3 (1983), pp. 462–471.
- [28] Y. Chen, M. Jankovic, M. Santillo, and A. D. Ames. “Backup Control Barrier Functions: Formulation and Comparative Study”. *Proc. IEEE Conf. Decision and Control*. 2021, pp. 6835–6841.
- [29] K.-C. Hsu, D. P. Nguyen, and J. F. Fisac. “ISAACS: Iterative Soft Adversarial Actor-Critic for Safety”. *Learning for Dynamics & Control*. Vol. 211. Proceedings of Machine Learning Research. June 2023.
- [30] R. Isaacs. “Differential Games I: Introduction”. *Differential Games I* (1954).
- [31] K.-C. Hsu, V. Rubies-Royo, C. J. Tomlin, and J. F. Fisac. “Safety and Liveness Guarantees through Reach-Avoid Reinforcement Learning”. *Proc. Robotics: Science and Systems*. July 2021.
- [32] B. Thananjeyan, A. Balakrishna, S. Nair, et al. “Recovery RL: Safe Reinforcement Learning With Learned Recovery Zones”. *IEEE Robotics and Automation Letters* 6.3 (2021), pp. 4915–4922.
- [33] O. Bastani. “Safe Reinforcement Learning with Non-linear Dynamics via Model Predictive Shielding”. *Proc. American Control Conference*. 2021, pp. 3488–3494.
- [34] T. Haarnoja, A. Zhou, P. Abbeel, and S. Levine. “Soft Actor-Critic: Off-Policy Maximum Entropy Deep Reinforcement Learning with a Stochastic Actor”. *Int. Conf. Machine Learning*. Vol. 80. Proceedings of Machine Learning Research. July 2018, pp. 1861–1870.
- [35] E. Vinitzky, Y. Du, K. Parvate, K. Jang, P. Abbeel, and A. Bayen. “Robust Reinforcement Learning using Adversarial Populations”. 2020.
- [36] E. Coumans and Y. Bai. “PyBullet, a Python module for physics simulation for games, robotics and machine learning”. <http://pybullet.org>. 2016–2021.